공학석사 학위논문

New metal redox battery system using hybrid electrolyte

삼중 전해질을 이용한 새로운 금속 레독스 전지 시스템에 관한 연구

2014년 2월

서울대학교 대학원

재료공학부

배 영 준

New metal redox battery system using hybrid electrolyte

삼중 전해질을 이용한 새로운 금속 레독스 전지 시스템에 관한 연구

지도교수 강 기 석

이 논문을 공학석사 학위논문으로 제출함

2014년 1월

서울대학교 대학원

재료공학부

배 영 준

배 영 준의 석사학위논문을 인준함

2014년 1월

위 원 장 남 기 태 (인)

부 위 원 장 강 기 석 (인)

위 원 장 호 원 (인)

Abstract

New metal redox battery system using hybrid electrolyte

Bae, Youngjoon

Department of Material Science and Engineering

College of Engineering

The Graduate School

Seoul National University

Li-aqueous batteries are innovative system that solve problem of traditional aqueous batteries. Aqueous batteries have many merits like safety, economic feasibility, and various cell reaction. However, cell voltage of aqueous batteries are low because electrochemical stability window of H_2O is narrow (0~1.23 V *vs.* SHE). For this reason, aqueous batteries are rarely used and non-aqueous Li-ion batteries are commercialized today. Li-aqueous batteries are new concept that can increase the voltage of aqueous battery. We constructed this Li-aqueous battery system and tested the cell using attractive

redox system. $Ni^{2+}/Ni_{(s)}$ redox reaction contain two electron for one transition metal, resulting in large specific capacity. Fe^{3+}/Fe^{2+} redox reaction has high voltage (3.81 V *vs.* Li^{+}/Li) and iron sources are inexpensive. We also analyzed the cell reaction by XRD, SEM, and GITT analysis. By this new metal redox battery system using hybrid electrolyte, we obtained large capacity of $Ni^{2+}/Ni_{(s)}$ reaction and high voltage of Fe^{3+}/Fe^{2+} reaction.

Keywords: Li-aqueous battery; Ni-Li battery; Fe-Li battery; New cell system; Various cell reactions

Student Number: 2012-20603

Contents

List of Figures

Chapter 1. Introduction

1.1 Motivation

Recently, non-aqueous lithium rechargeable batteries have been researched very intensely because of its high power and energy density. Current demand for portable device, electric vehicle, and energy storage system shows that non-aqueous lithium rechargeable batteries are the best candidates to keep the high performance. However, cathode materials for non-aqueous lithium rechargeable battery are commonly limited to crystal structures in which intercalation/deintercalation reactions can be occur. Instead, cathode materials for aqueous battery are various and have been researched for a long time.[1]

Looking back to history of batteries, the invention of lead-acid battery which is the first practical rechargeable battery was developed by G. Plante in 1859. At that time, electric vehicles were powered by lead-acid batteries. After combustion-engine was developed in 1910, electric vehicles that contain lead-acid batteries were almost disappeared. Instead, lead-acid batteries have been used as SLI(starting, lighting, ignition) and stationary emergency power. As the second rechargeable battery, nickel-cadmium batteries were developed by Jungner of Sweden in 1899. In the 1940s, as sealed nickel cadmium battery were available, markets for portable devices and military equipment

were created. After that, many aqueous batteries such as nickel-metal hydride, zinc-manganese dioxide, zinc-air batteries were developed. [1]

Lithium batteries that contain non-aqueous electrolyte, have undergone two generations since it appeared. The first generation is commercialization of primary lithium batteries. The second one is development of rechargeable lithium batteries. depletion of oil resources and environmental problems have provoked attention in renewable energy sources. Among various renewable energy sources, performances of lithium rechargeable batteries are excellent due to their high energy density and specific energy as shown in Figure 1.1.[2] Lithium rechargeable batteries exhibits specific energy about 150 Wh/kg, which is higher than aqueous batteries.

As shown above, non-aqueous lithium batteries have high energy density, and aqueous batteries have a lot of cathode materials. Because lithium metal reacts with H_2O intensely, aqueous electrolytes are hardly used in lithium batteries. Therefore, non-aqueous lithium batteries cannot use various cathode reaction that are available in aqueous batteries. Traditional cathode materials for lithium batteries are confined to lithium insertion materials, so developments of cathode materials were limited. If we can use aqueous cathode materials in lithium batteries, we extend the range of cathode materials. In this research, we adopt aqueous electrolyte to lithium battery to extend its range of cathode materials.

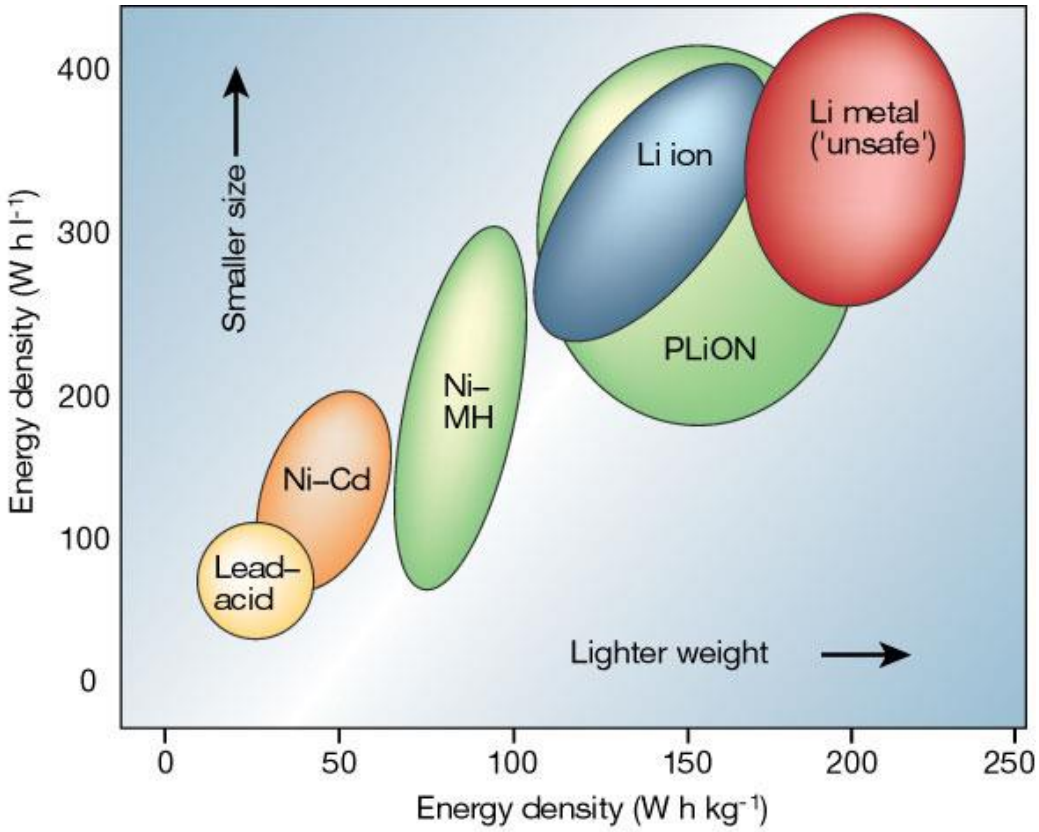

Figure 1.1 Comparison of the different battery technologies in terms of volumetric and gravimetric energy density.

1.2 Related Research Trends

To adopt aqueous electrolyte to lithium batteries, lithium metal avoid direct contact with H_2O. For separation lithium metal from H_2O, solid electrolyte which conduct lithium ion is necessary. Lithium ion conducting solid electrolytes have been researched long time, and among various solid electrolyte, LATP ($Li_{1+x+y}Al_xTi_{2-x}Si_yP_{3-y}O_{12}$) is stable in water and non-aqueous electrolyte.[3] Additionally, LATP has good lithium ion conductivity. (about 10^{-4} S/cm at room temperature)[3] With LATP solid electrolyte, lithium metal can be successfully separated from aqueous electrolyte. After solid electrolyte can be got commercially, many researches related to aqueous lithium batteries have been done. Representatively, Aqueous lithium air batteries are developed for recent years.[4-13] Non-aqueous lithium air batteries are actively researched because of its extremely high energy density.[14-30] But low reversibility of discharge products (Li_2O_2) which clog pores of cathode materials and accumulate during cycling deteriorate the performance of lithium air batteries. On the other hand, discharge products of aqueous lithium air batteries (LiOH, H_2O) don't clog pores or accumulate on cathode materials. For this reason, aqueous lithium air batteries has better cycle life than non-aqueous lithium air batteries theoretically. Besides aqueous lithium air batteries, new concept of nickel-lithium battery or zinc-potassium permanganate battery was suggested. [31, 32]

1.3 Research purpose

For realization of aqueous lithium batteries, solid electrolyte that separate lithium metal and aqueous electrolyte is necessary. Commercially, cell system to which solid electrolyte is applicable is not exist. Therefore, we should design the cell system first. After optimization of the cell system, we will test our strategic cell reaction.

Generally, high capacity, high voltage, and economical materials are demanded for a good battery system. High capacity and high voltage mean that battery has high energy density, and economical materials are necessary for mass production. In this study, we have two strategy. First, If we use multi electron reaction per one transition metal, we can get several times of capacity theoretically. We elect $Ni^{2+}/Ni_{(s)}$ redox reaction as this multi electron reaction per one transition metal because this reaction has proper voltage to use in the aqueous electrolyte. Second, we use Fe^{3+}/Fe^{2+} redox which is economical, and has high redox voltage of 0.77 V *vs.* SHE. Here, we show that our cell system is well designed. Next, we construct new lithium aqueous cell system using $Ni^{2+}/Ni_{(s)}$ and Fe^{3+}/Fe^{2+} redox reaction to get more capacity, and high voltage with economical price.

Chapter 2. Research backgrounds

2.1 Lithium Rechargeable Batteries

Recently, demands for portable devices are increased, and renewable energies such as photovoltaic, wind energy, and geothermal energy are demanded as oil resources have been exhausted. To use high technology portable devices, rechargeable batteries that have high energy density and power capability are necessary. In the case of renewable energy, energy storage is very important because energy productions and energy consumptions occur at different times. To store renewable energy, large scale energy storage systems which are composed of rechargeable batteries are needed. For this reason, rechargeable batteries that have high energy density and power capability have been researched intensely. Among various rechargeable batteries, performances of lithium rechargeable batteries are superior as shown in Figure 1.1. Discharge voltage and energy density of lithium rechargeable batteries are around 3.7 V and 150 Wh kg^{-1}, respectively, which are much higher than those of other rechargeable batteries.

Basic principle of lithium rechargeable batteries is shown in Figure 2.1 Lithium rechargeable batteries are composed of anode, electrolyte, cathode, and separator. During discharge, lithium ions diffuse from anode to cathode through the electrolyte and electrons move from anode to cathode through an external circuit spontaneously, because

lithium ions at cathode crystal structure are more stable than that at anode. During charge, lithium ions and electrons move back to anode, and this process need electric energy because charge process is not spontaneous. Electric energy is saved as chemical energy in the batteries during charge, and chemical energy is converted to electric energy during discharge.

In conventional Li rechargeable battery, $LiCoO_2$ is used as a cathode, and graphite is used as an anode. The electrochemical reaction during discharge/charge are expressed as follow:

Anode reaction: $Li_xC_6 = xLi+ + xe- + C_6$

Cathode reaction: $Li_{1-x}CoO_2 + xLi+ + xe- = LiCoO2$

The energy that can be stored in the battery is determined by the specific capacity and operation voltage. The specific capacity indicate the amount of electron that move from anode to cathode per unit weight, and the operation voltage is determined by the difference in the chemical potential of lithium ion between the cathode and anode.

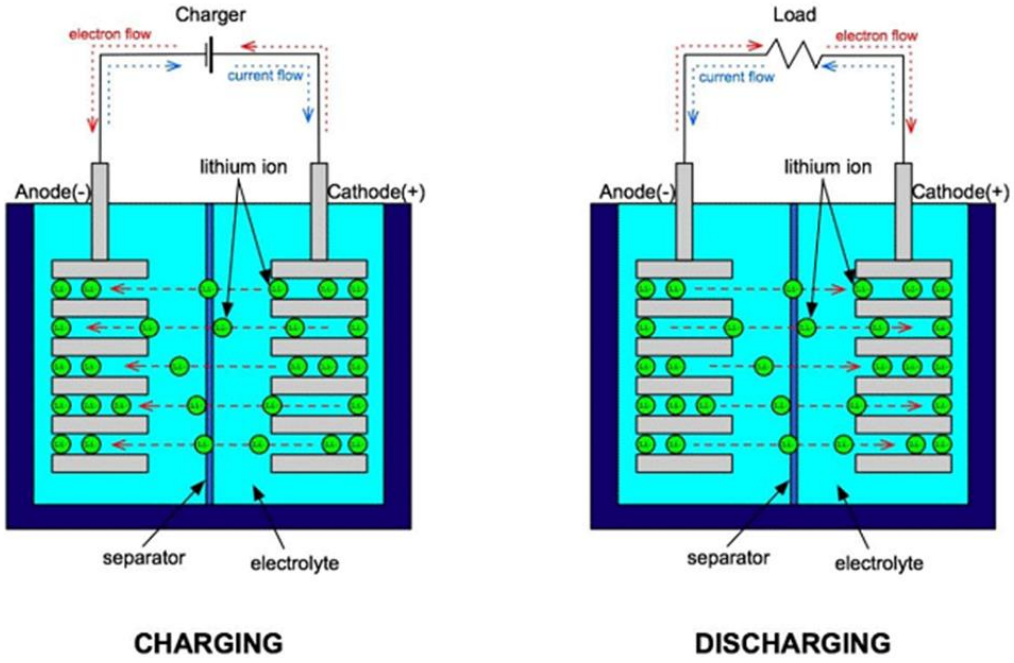

Figure 2.1 Schematic figure for the fundamental of lithium rechargeable battery.

2.2. Lead-Acid Battery

Lead-acid battery was developed in 1859 by Gaston Planté. It consist of cathode material as PbO_2, anode material as $Pb_{(s)}$, and electrolyte as aqueous H_2SO_4. During discharge, both the cathode and anode materials become lead sulfate ($PbSO_4$) and the electrolyte loses sulfuric acid. The electrochemical cell reactions are as follow:

$$\text{Anode reaction: } Pb_{(s)} + HSO_{4(aq)} = PbSO_{4(s)} + H^{+}_{(aq)} + 2e$$

$$\text{Cathode reaction: } PbO_{2(s)} + HSO_{4(aq)} + 3H^{+}_{(aq)} + 2e = PbSO_{4(s)} + 2H_2O_{(l)}$$

$$\text{Overall reaction: } Pb_{(s)} + PbO_{2(s)} + 2H_2SO_{4(aq)} = 2PbSO_{4(s)} + 2H_2O_{(l)}$$

Theoretically a cell can produce two faradays of charge (192,971 coulombs) from 642.6 g of reactants. At 2 volts per cell, this comes to 167 Wh kg^{-1}, but lead-acid batteries actually give only 30 to 40 Wh kg^{-1} due to the weight of other constituents. When lead acid battery undergo overcharging, oxygen and hydrogen gas can be produced by electrolysis of water, and that is loss of electrolyte. For this reason, valve regulated lead acid battery (VRLA) have been used commonly. In the VRLA, oxygen and hydrogen that produced during overcharging can recombine into water. Main applications of lead acid batteries are automobile starting, lighting and ignition (SLI) batteries, grid energy storage, and household electric power systems. [33]

2.3. Nickel-Lithium battery

Rechargeable Nickel-Lithium battery (Ni-Li battery) was first invented by Haoshen Zhou's research group.[31] The components of this Ni-Li battery are lithium metal, organic electrolyte (1 M $LiClO_4$ in ethylene carbonate/dimethyl carbonate), Li ion conducting solid electrolyte (LISICON), aqueous electrolyte (1 M LiOH and 1 M KOH), and $Ni(OH)_2$ cathode. Electrochemical cell reactions are as follow:

Anode reaction : $Li^+ + e = Li$ (E = -3.04 V *vs.* SHE)

Cathode reaction : $Ni(OH)_2 + OH^- = NiOOH + H_2O + e$ (E = 0.49 V *vs.* SHE)

Overall reaction : $Ni(OH)_2 + LiOH = NiOOH + Li + H_2O$ (E = 3.53 V)

During charge, $Ni(OH)_2$ is converted to NiOOH and Li ions diffuse from the aqueous electrolyte to organic electrolyte through a LISICON film and reduced to lithium metal at anode. The discharge process is reverse one. In this system, high theoretical voltage of 3.53 V is possible because standard reduction potential of Li^+/Li is very low. Conventional aqueous battery has low voltage because electrochemical stability window of water is narrow. (0~1.23 V *vs.* SHE) Unlike conventional aqueous battery, aqueous electrolyte of Ni-Li battery is only in the cathode part. Therefore, reduction of water does not occur even though standard reduction potential of anode reaction is lower than 0 V. For this reason, by using Li^+/Li anode reaction that has extremely low standard reduction potential, high voltage could be obtained in this cell system. The cell configurations of Li-ion battery, Ni-MH battery, and Ni-Li battery are compared in Figure 2.2

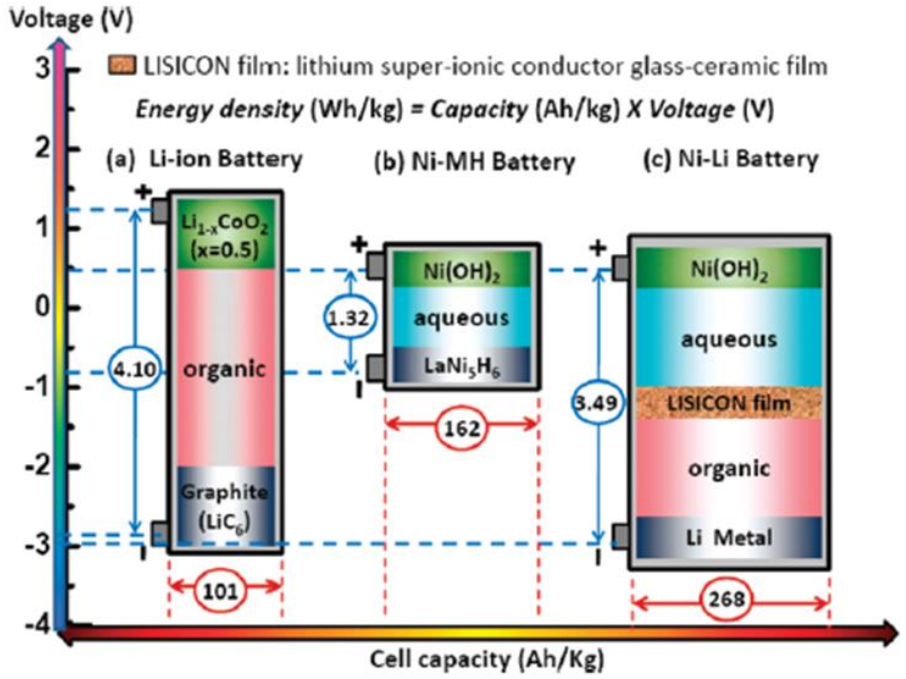

Figure 2.2 Key components, cell voltage, and cell capacity of Li-ion battery, Ni-MH battery, and Ni-Li battery.

Chapter 3. Experimental section

3.1 Cell Design and Fabrication

For electrochemical cell test, we should design and fabricate the cell in which non-aqueous electrolyte, solid electrolyte, and aqueous electrolyte can be put. Therefore we designed the cell first. Figure 3.1 is the schematic of our cell design. If lithium metal directly contact with aqueous electrolyte, intense reaction would occur between lithium metal and water. The reaction is shown below.

$$2Li_{(s)} + 2H_2O_{(l)} = 2LiOH_{(aq)} + H_{2(g)}$$

Therefore, lithium metal should be separated from aqueous electrolyte. To separate lithium metal from aqueous electrolyte, we put solid electrolyte between lithium metal and aqueous electrolyte. Designed cell is composed of two part. Aqueous electrolyte is put in the upper part whereas lithium metal is put in the lower part. Solid electrolyte is between two parts to separate lithium metal from aqueous electrolyte.

Generally, contact between solid and solid is not perfect, so contact between lithium metal and solid electrolyte is not perfect. This lower ionic conductivity at the boundary seriously, and increase cell resistance to drop cell voltage. Also, Direct contact of lithium metal and commonly used solid electrolyte, LATP lead to a deterioration of

LATP because of strong reducing power of lithium metal. Therefore something should be put in between lithium metal and solid electrolyte. We used non-aqueous electrolyte to keep lithium metal from solid electrolyte. This construction is well drawn in Figure 3.1. Based on this schematic, we fabricate cell for electrochemical test. Figure 3.2 shows digital photograph of fabricated cell.

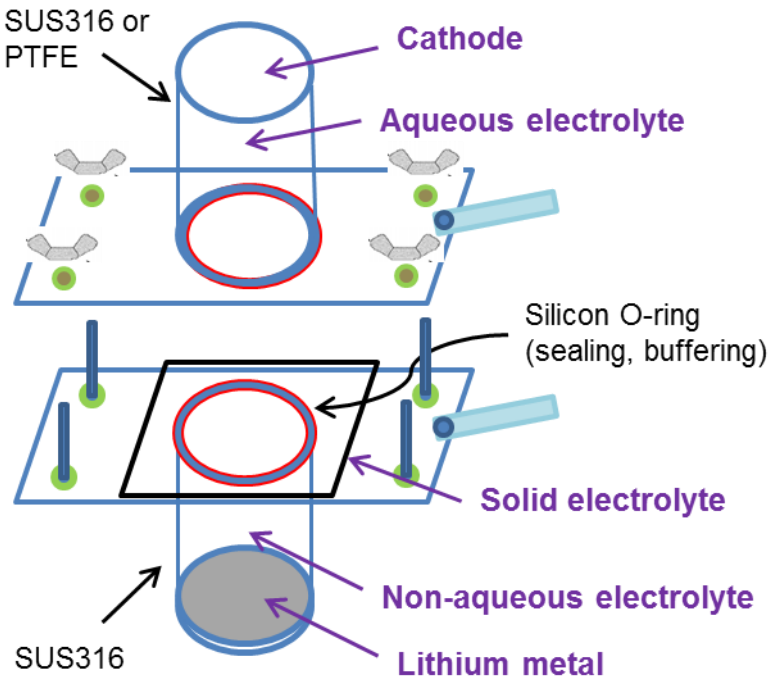

Figure 3.1 Schematic of cell design

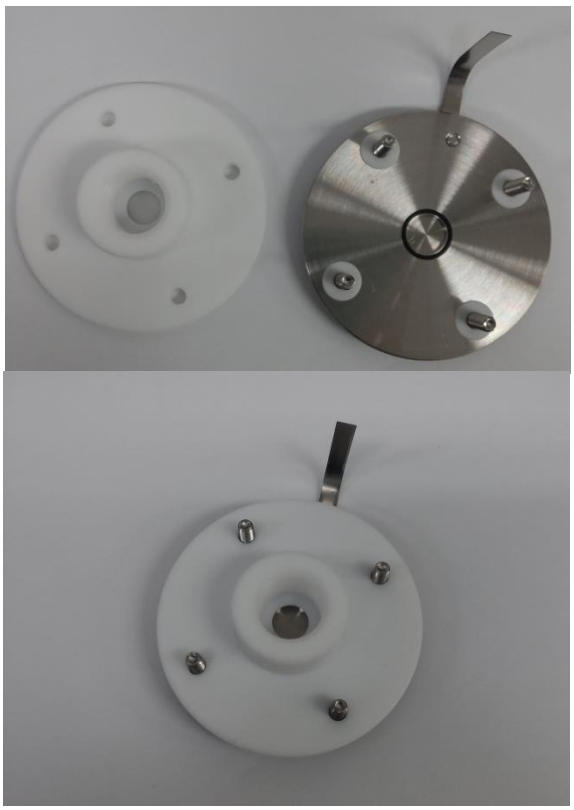

Figure 3.2 Digital photograph of fabricated cell for electrochemical test

3.2 Cathode Electrode Fabrication

Cathode electrodes were prepared by casting a mixture of Ketjen black (EC 600JD, Ilshin Chemtech), catalyst, and Kynar 2801 as a binder. The electrode was formed with KB and kynar 2801 at a weight ratio of 80:20. The mixture were dispersed in N-methyl-2-pyrrolidone (NMP, Sigma-Aldrich, 99.5%) and then pasted onto the Ni mesh (3/8 inch diameter), which was used as a current collector. Finally, the mixture was heated at 120 ^{o}C for 12 hour to evaporate NMP.

3.3 Cell Assembly

Lithium (3/8 inch diameter) was used as a counter electrode. The non-aqueous electrolyte was a 1M solution of $LiPF_6$ dissolved in a mixture of ethylene carbonate (EC), and dimethyl carbonate (DMC) (1:1 v/v). LATP ($Li_{(1+x+y)}Al_xTi_{2-x}Si_yP_{(3-y)}O_{12}$) solid electrolyte (Ohara Corporation, 0.15 mm in thickness) was put on the non-aqueous electrolyte, and then fixed with upper part of cell by screw. This fixing procedure was done in an argon atmosphere glove box. After fixing solid electrolyte, 0.2 mL of Aqueous electrolyte was dropped on the solid electrolyte. Then cathode material was put on aqueous electrolyte. For Ni-Li battery using $Ni^{2+}_{(aq)}/Ni_{(s)}$ redox reaction, we used aqueous electrolyte of 0.5 M $(CH_3COO)_2Ni$ + 0.5 M $LiNO_3$ in deionized (DI) water. Also, Aqueous electrolyte for Fe-Ni battery using $Fe^{3+}_{(aq)}/Fe^{2+}_{(aq)}$ redox reaction was 0.5 M $Fe(NO_3)_3$ + 0.05 M $LiNO_3$ in DI water.

3.4 Sample Characterization

The characterization of the samples were done using an X-ray diffractomerter (XRD, Rigaku, D/MAX-RB diffractometer, Tokyo, Japan) equipped with Cu Ka radiation by step scanning in the 2theta range of 10-90 ^{o}. The size and morphology of the products were observed by a field emission scanning electron microscope (FE-SEM, Carl Zeiss, SUPRA 55VP, Germany).

3.5 Electrochemical Test

The electrochemical test was carried out in ambient air by a potentio-galvanostat (Won A Tech, WBCS 3000, Korea). The charge/discharge profiles were measured at current densities of 0.4 and 1 mA cm^{-2} between 2.0-4.8 V and 3.05-4.8 V versus Li^{+}/Li, and all of the specific capacities are described in per gram units of transition metal weight.

Chapter 4. Result and discussion

4.1 Nickel-Lithium batteries using $Ni^{2+}_{(aq)}/Ni_{(s)}$ redox reaction

4.1.1 Electrochemical analysis

In the $Ni^{2+}_{(aq)}/Ni_{(s)}$ redox reaction, expected electrochemical reaction is as follow.

Anode reaction: $Li = Li^{+} + e^{-}$ (E = 3.04 V *vs.* SHE)

Cathode reaction: $Ni^{2+}_{(aq)} + 2e^{-} = Ni_{(s)}$ (E = -0.25 V *vs.* SHE)

Overall reaction : $2Li + Ni^{2+}_{(aq)} = 2Li^{+} + Ni_{(s)}$ (E = 2.79V)

During discharge, Ni^{2+} would be precipitated to $Ni_{(s)}$ in the cathode substrate which has high surface area because of ketjenblack carbon. After charge, precipitated $Ni_{(s)}$ would be oxidized and dissolved to Ni^{2+}. First discharge-charge profile is shown in Figure 4.1a. The first discharge capacity was 718 mAh g^{-1}, which is 78.6% of theoretical capacity of 913 mAh g^{-1}. As our strategy, the discharge capacity was high because two electron was used per one transition metal ion (Ni^{2+}). But the charge capacity was 85 mAh g^{-1} and overpotential was high, indicating charging process was very resistive. Theoretically, electro-conductivity of nickel metal which is discharge product of this cell

system is high. Therefore resistivity of discharged cell should be low, and overpotential during charge should also be small. But in our cell system, the result was completely opposite of expected one. This imply that during discharge to 718 mAh g^{-1}, side reaction that formed resistive products occurred. After full discharge to 2.0 V, the cathode electrode was covered with thick green film as shown in Figure 4.2. In the aqueous system, H_2O always exist and O_2 gas could flowed in the cell during cell assembly. Then $Ni_{(s)}$ could react with H_2O and O_2 to form $Ni(OH)_2$ or NiOOH which are very resistive compared to Ni metal. To reduce resistive side products and lead to our intended cell reaction, we tested the cell with capacity limitation of 85 mAh g^{-1}. Figure 4.1b shows the discharge-charge profile limiting capacity to 85 mAh g^{-1}. By capacity limitation, charging voltage was lowered and next discharge could be possible. But still, charging voltage was high and the discharge voltages were slightly reduced as cycles go on. This means that cell resistivity increased when discharge-charge process conducted. Despite of low capacity of 85 mAh g^{-1}, side reaction could occur and resistive products could pile up after discharge-charge process.

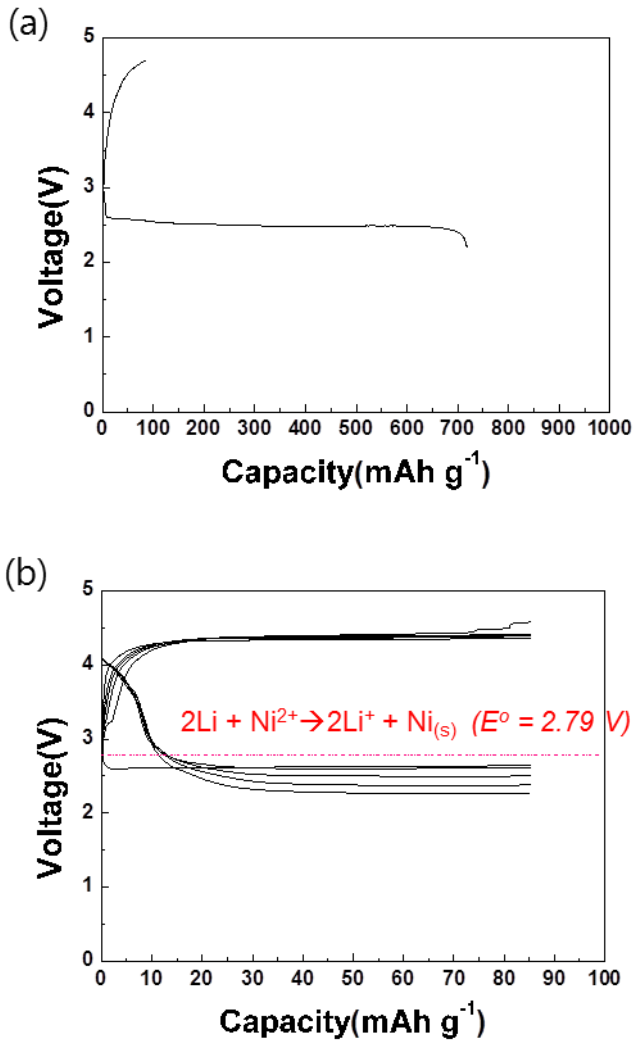

Figure 4.1 Electrochemical profile of Ni-Li battery using $Ni^{2+}_{(aq)}/Ni_{(s)}$ redox reaction

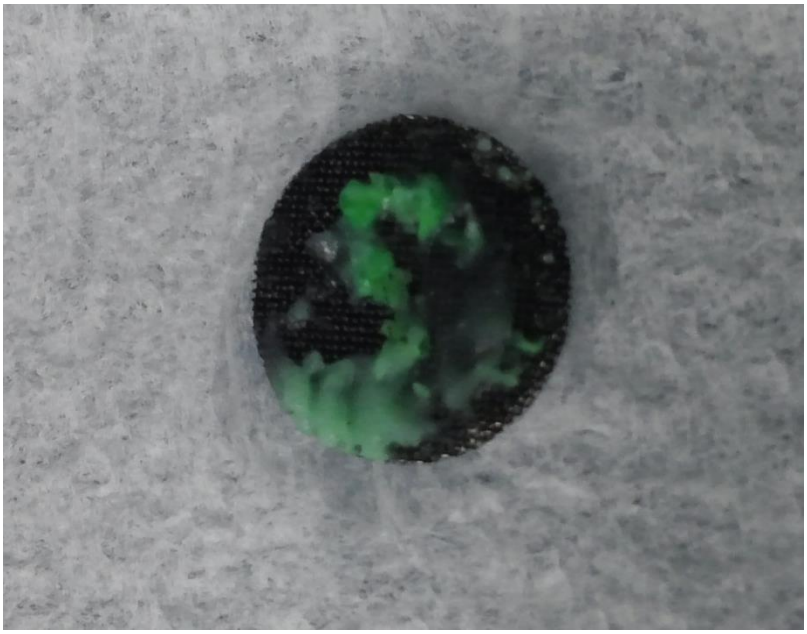

Figure 4.2 Cathode electrode after full discharge to 2.0 V

4.1.2 XRD and SEM analysis

By limiting capacity to 85 mAh g^{-1} and minimizing side reaction, the cell could be charged well and worked for 5 cycles. We analyzed the discharge products to confirming the cell reaction using XRD and SEM. We expected that Ni^{2+} would be reduced to $Ni_{(s)}$ and precipitated on the cathode electrode. Therefore, we analyzed XRD peaks for three samples which are as prepared, after discharge to 85 mAh g^{-1}, and after charge to 85 mAh g^{-1}. For detecting nickel, we used aluminum foil as current collector. XRD results are shown in Figure 4.3. As prepared sample showed only aluminum peak and amorphous carbon peak below 30 ^{o}. After discharge, we observed Ni peaks at 51.4 and 76.2 ^{o}. Ni peak at 44.8^{o} was overlap with Al peak. After discharge, Al peak also changed because ketjenblack was peeled off from Al foil during discharge and Al surface was more exposed to X-ray than that of as prepared sample. After discharge, Ni was produced as discharge product as we expected and this result accord with our strategy to use two electron per on Ni^{2+} ion. Although side reaction could be occur, main discharge product is Ni. After charge, Ni peaks at 51.4 and 76.2 ^{o} were almost disappeared indicating that precipitated Ni metal oxidized to Ni^{2+}. From this XRD result, we noticed that reversible $Ni^{2+}/Ni_{(s)}$ redox reaction was occurred during discharge and charge process.

We also observed surface of ketjenblack on Ni mesh which is cathode electrode to check the morphology of discharge products. Figure 4.4 shows the SEM images of samples which are as prepared, after discharge to 85 mAh g^{-1}, and after charge to 85 mAh g^{-1}. Fig 4.4a shows that porous surface of ketjenblack. Particle size of Ketjenblack is

about 10~20 nm and ketjenblack particles are well dispersed on Ni mesh. Fig 4.4b shows the surface of ketjenblack after discharge to 85 mAh g^{-1}. Thin film was produced on the surface of ketjenblack and we already identify this discharge product as Ni using XRD spectra. Discharge product has film morphology and this film covered all the surface of ketjenblack. After charge, the film like discharge product was clearly disappeared and surface of porous ketjenblack was observed again as shown in Figure 4.4c. This SEM images correspond with XRD results. After discharge, film like Ni was produced and this discharge product disappeared after charge.

From XRD and SEM images, we clearly noticed that $Ni^{2+}/Ni_{(s)}$ redox reaction occurred during discharge-charge process. Also we find that Ni was produced in the form of film morphology. This result imply that surface area of cathode substrate have direct effect on discharge capacity. Therefore, design for large surface area is important work to increase the discharge capacity.

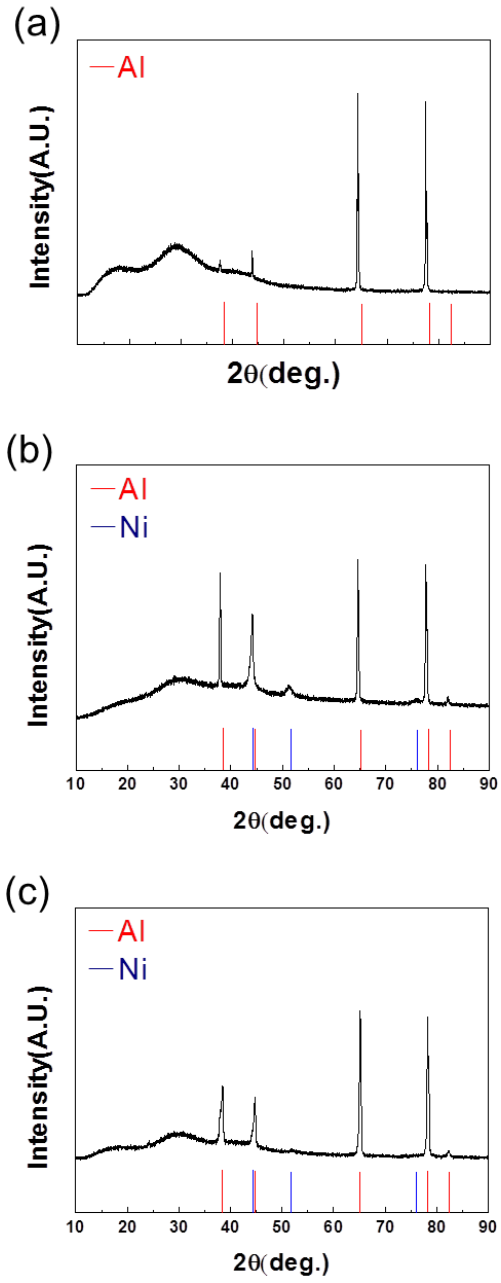

Figure 4.3 XRD spectra of cathode electrode (a) as prepared, (b) after discharge, (c) after charge

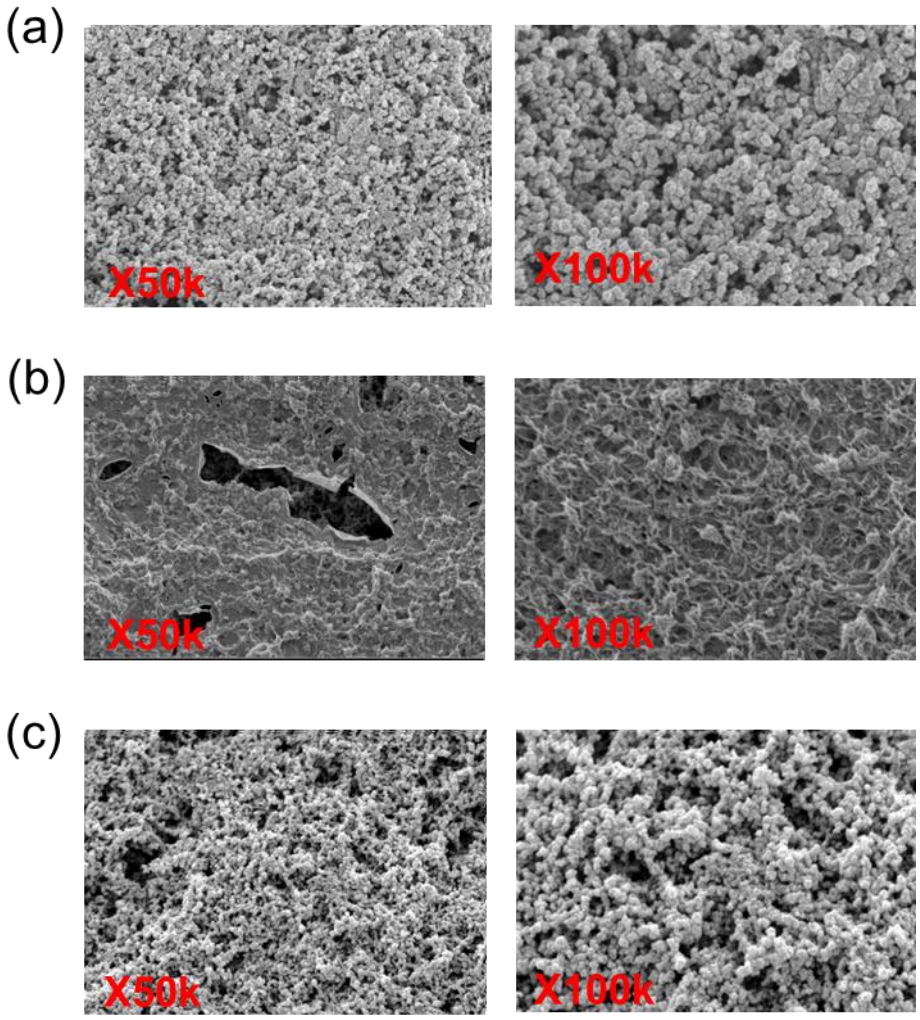

Figure 4.4 SEM images of cathode electrode (a) as prepared, (b) after discharge, (c) after charge

4.2 Iron-Lithium batteries using $Fe^{3+}_{(aq)}/Fe^{2+}_{(aq)}$ redox reaction

4.2.1 GITT (galvanostatic intermittent titration technique) analysis

Our second strategy was making the new system that contain economical transition metal and show high voltage for high energy density. We select $Fe^{3+}_{(aq)}/Fe^{2+}_{(aq)}$ redox reaction because this redox have high voltage of 3.81 V *vs.* Li^+/Li and iron is economical transition metal. Before analyze the electrochemical properties of this cell system, we conducted GITT analysis to check $Fe^{3+}_{(aq)}/Fe^{2+}_{(aq)}$ redox reaction. Figure 4.5 shows the GITT analysis of $Fe^{3+}_{(aq)}/Fe^{2+}_{(aq)}$ redox system. The expected cell reaction is as below.

Anode reaction: $Li = Li^+ + e^-$ (E = 3.04 V *vs.* SHE)

Cathode reaction: $Fe^{3+}_{(aq)} + e^- = Fe^{2+}_{(aq)}$ (E = 0.77 V *vs.* SHE)

Overall reaction: $Li + Fe^{3+}_{(aq)} = Li^+ + Fe^{2+}_{(aq)}$ (E = 3.81V)

The voltage of overall reaction (3.81 V) is marked with red line in Figure 4.5. During discharge and charge, the cell voltage is apart with theoretical voltage (3.81 V) of cell reaction because of overpotential caused by resistivity. However, during rest for 1h, the cell voltage (3.81 V) is close to theoretical voltage of cell reaction for all rest times.

Rest voltages are not exactly matched with 3.81 V because theoretical voltage is changed with pH variation. From this result, we clearly noticed that $Fe^{3+}_{(aq)}/Fe^{2+}_{(aq)}$ redox reaction occur during discharge-charge process.

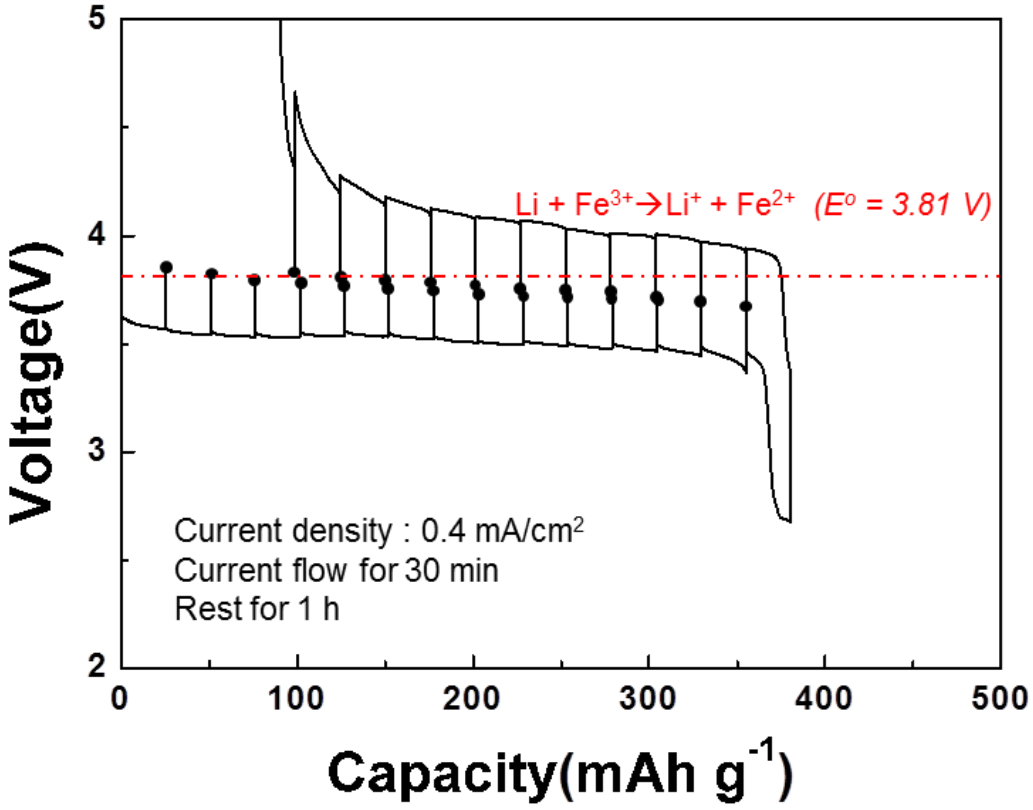

Figure 4.5 GITT analysis of $Fe^{3+}_{(aq)}/Fe^{2+}_{(aq)}$ redox system

4.2.2 Electrochemical properties

Figure 4.6a shows the discharge-charge profile of $Fe^{3+}_{(aq)}/Fe^{2+}_{(aq)}$ redox system. Theoretical capacity of this system is 480 mAh g^{-1}. For first discharge, 66% of theoretical capacity (310 mAh g^{-1}) was obtained. But only 125 mAh g^{-1} was obtained from first charge process. Discharge and charge voltages were closed to theoretical voltage of this cell system (3.81 V). After charge to 125 mAh g^{-1}, the cell voltage sharply increased and the cell operation ended because of voltage cut (4.8 V). 66% of theoretical capacity during first discharge indicating that all of the Fe^{3+} ions didn't participate in the cell reaction. The diffusion of Fe^{3+} could not be enough resulting in increase in cell resistivity and capacity fading. After discharge, 66 % of Fe^{3+} ions are reduced to Fe^{2+} ions. However, during charge, only 40 % of produced Fe^{2+} ions participated in the electrochemical reaction. During 2^{nd} and 7^{th} cycles, the capacities were closed to 125 mAh g^{-1} resulting in almost 100% of coulombic efficiency.

From this cell system, we obtained high discharge voltage of about 3.6 V using economical iron source as our strategy. But capacity loss during 1^{st} cycle was serious problem of this cell system. After first irreversible capacity, cell capacities during 2^{nd} ~7^{th} cycles are similar, indicating that side reactions were occurred during 1^{st} cycle. This side reaction could occur because of variation of pH value during discharge process. pH value of 0.5 M Fe^{3+} ions is 1.22 and that of 0.5 M Fe^{2+} is 6.05. Theoretically, pH value changes from 1.22 to 6.05 during full discharge. At pH 2.0, Fe^{2+} react with O_2 gas and H_2O to form FeO(OH) and at pH 4.48, $Fe(OH)_3$ could be precipitated. Therefore, during

discharge, Fe^{2+} ions were produced and pH value increased, and at the point of pH value of 2.0, produced Fe^{2+} participate in side reaction. After full discharge to 3.05 V, Fe^{3+} ions that didn't participate in cell reaction, Fe^{2+} ions as discharge products, and byproducts like FeO(OH) and $Fe(OH)_3$ could be exist in the aqueous electrolyte. Because Fe^{2+} ions are consumed in the side reactions, 1st charge capacity reduced to 125 mAh g^{-1} which is 40% of 1st discharge capacity. After 1st cycle, side reactions did not occur, and discharge and charge capacities of 2nd ~7th cycle maintained about 125 mAh g^{-1}.

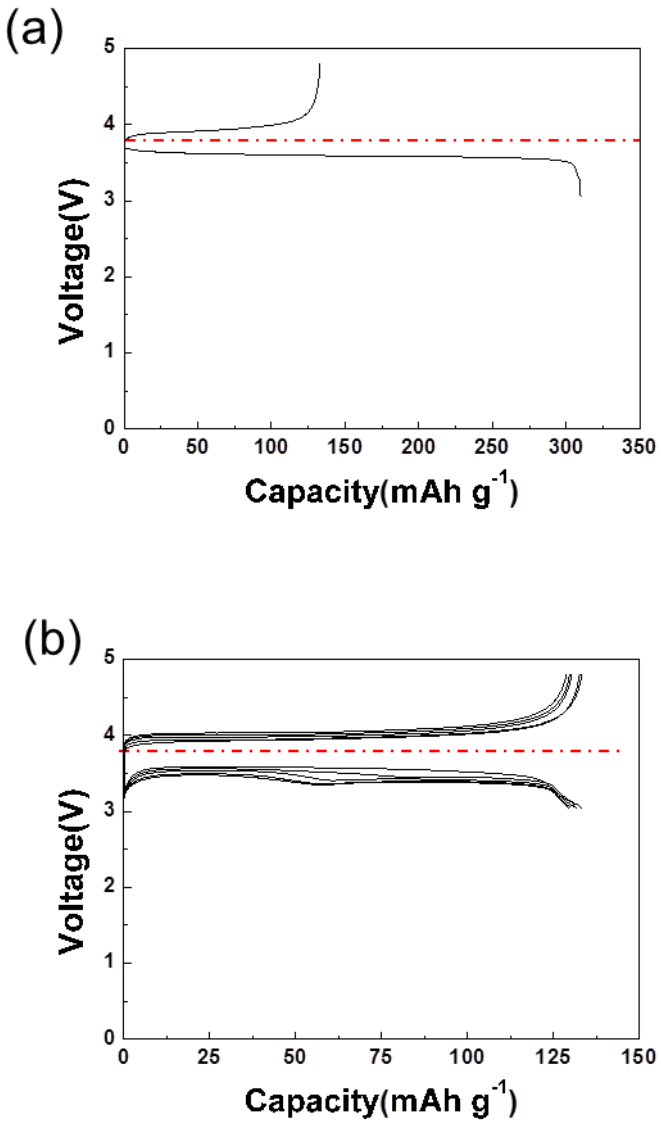

Figure 4.6 Electrochemical profile Fe-Li battery using $Fe^{3+}_{(aq)}/Fe^{2+}_{(aq)}$ redox system, (a) 1st cycle (b) 2nd ~7th cycles

Chapter 5. Conclusion

We successfully design new cell system that contain hybrid electrolyte. Using this cell design, we construct Li-aqueous battery. Our strategy is as follow. First, multi-electron reaction per one transition metal will increase the cell capacity resulting in increased energy density. We select $Ni^{2+}/Ni_{(s)}$ redox reaction to realize our strategy. Second, high voltage redox reaction of economical transition metal will not only increase energy density, but also reduce economic problem for making large scale energy storage system. We select Fe^{3+}/Fe^{2+} redox system because this redox voltage is high (3.81V vs. Li^{+}/Li), and cheap iron sources are used in cell system. For the $Ni^{2+}/Ni_{(s)}$ redox system, the cell showed high capacity of 718 mAh g^{-1} as our strategy. But charging process was very resistive and charging voltage was increased sharply resulting in negligible charge capacity. During long discharge, resistive byproducts like nickel hydroxide could be produced and this byproducts increased the cell resistivity. To minimize side reaction and identify the cell reaction, we tested the cell with capacity limitation of 85 mAh g^{-1}. After limiting capacity, 5 cycles could be obtained. $Ni^{2+}/Ni_{(s)}$ redox reaction was analyzed by XRD and SEM images. For Fe^{3+}/Fe^{2+} redox system, the cell showed high voltage of 3.6 V which is close to theoretical voltage of the cell (3.81 V). At first 1^{st} cycle, irreversible capacity was observed. The reason of this irreversible capacity was precipitation of FeO(OH) and $Fe(OH)_3$ due to pH variation during discharge process. After 1^{st} cycle, the cell was stabilized and showed nearly 100 % of coulombic efficiency. From our research, we find the possibility of new cell system that has large capacity or high voltage.

Although many problems remained in our cell system, this Li-aqueous battery system is very attractive because various redox reactions could be used in aqueous system.

Reference

[1] F. Beck,, P. Ruetschi, *Electrochim. Acta* **2000**, 45, 2467

[2] M. Armand, J. M. Tarascon, *Nature* **2008**, *451*, 652.

[3] L. Puech, C. Cantau[a], P. Vinatier[a], G. Toussaint, P. Stevens, *J. Power Sources* **2012**, 214, 330

[4] T. Zhang, N. Imanishi, Y. Shimonishi, A. Hirano, J. Xie, Y. Takeda, O. Yamamoto, N. Sammes, *J. Electrochem. Soc.* **2010**, 157, A214

[5] L. Li, A. Manthiram, *J. Mater. Chem. A* **2013**, 1, 5121

[6] T. Zhang, N. Imanishi, S. Hasegawa, A. Hirano, J. Xie, Y. Takeda, O. Yamamoto, N. Sammes, *J. Electrochem. Soc.* **2008**, 155, A965

[7] P. He, Y. Wang, H. Zhou, *J. Power Sources* **2011**,196, 5611

[8] L. Li, X. Zhao, A. Manthiram, *Electrochem. Commun.* **2012**, 14, 78

[9] Y. Li, K. Huang, Y. Xing, *Electrochim. Acta* **2012**, 81, 20

[10] E. Yoo, H. Zhou, *ACS Nano* **2011**, 5, 3020

[11] T. Zhang, N. Imanishi, Y. Shimonishi, A. Hirano, Y. Takeda, O. Yamamoto, N. Sammes, *Chem. Commun*. **2010**, 46, 1661

[12] Y. Wang, H. Zhou, *J. Power Sources* **2010**, 195, 358

[13] H. He, W. Niu, N. M. Asl, J. Salim, R. Chena, Y. Kim, *Electrochim. Acta* **2012**, 67, 87

[14] K. M. Abraham, Z. Jiang, *J. Electrochem.Soc.* **1996**, 143, 1

[15] A. Debart, A. J. Paterson, J. Bao, P. G. Bruce, *Angew. Chem., Int. Ed.* **2008**, 47, 4521

[16] P. G. Bruce, S. A. Freunberger, L. J. Hardwick, J. M. Tarascon, *Nat. Mater.* **2012**, 11, 19

[17] J. Xiao, D. Mei, X. Li, W. Xu, D. Wang, G. L. Graff, W. D. Bennett, Z. Nie, L. V. Saraf, I. A. Aksay, J. Liu, J. G. Zhang, *Nano Lett*. **2011**, 11, 5071

[18] S. A. Freunberger, Y. Chen, N. E. Drewett, L. J. Hardwick, F. Bard, P. G. Bruce, *Angew. Chem. Int. Ed.* **2011**, 50, 1

[19] C. Ó Laoire, S. Mukerjee, E. J. Plichta, M. A. Hendrickson, K. M. Abraham, *J. Electrochem. Soc.* **2011**, 158, A302

[20] H. Wang, Y. Yang, Y. Liang, G. Zheng, Y. Li, Y. Cui, H. Dai, *Energy Environ. Sci.* **2012**, 5, 7931

[21] R. Black, S. H. Oh, J. H. Lee, T. Yim, B. Adams, L. F. Nazar, *J. Am. Chem. Soc.* **2012**, 134, 2902

[22] J. Gomez, E. E. Kalu, R. Nelson, M. H. Weatherspoonb, J. P. Zheng, *J. Mater. Chem. A*, **2013**, 1, 3287

[23] Y. Shen, D. Sun, L. Yu, W. Zhang, Y. Shang, H. Tang, J. Wu, A. Cao, Y. Huang, *Carbon*, **2013**, 6 2, 288

[24] J. Hassoun, H. G. Jung, D. J. Lee, J. B. Park, K. Amine, Y. K. Sun, B.

Scrosati, *Nano Lett.* **2012**, 12, 5775

[25] F. Li, H. Kitaura, H. Zhou, *Energy Environ. Sci.* **2013**, 6, 2302

[26] Y. C. Lu, Y. Shao-Horn, *J. Phys. Chem. Lett.* **2013**, 4, 93

[27] F. Li, T. Zhang, H. Zhou, *Energy Environ. Sci.* **2013**, 6, 1125

[28] B. M. Gallant, D. G. Kwabi, R. R. Mitchell, J. Zhou, C. V. Thompson, Y. Shao-Horn, *Energy Environ. Sci.* **2013**, 6, 2518

[29] Y. Chen, S. A. Freunberger, Z. Peng, O. Fontaine, P. G. Bruce, *Nat. Chem.* **2013**, 5, 489

[30] X. Guo, N. Zhao, *Adv. Energy Mater.* **2013**, 3, 1413

[31] H. Li, Y. Wang, H. Na, H. Liu, .H. Zhou, *J. Am. Chem. Soc*. **2009**, 131, 15098

[32] L. Chen, Z. Guo, Y. Xia, Y. Wang, *Chem. Commun.* **2013**, 49, 2204

[33] D. Linden, T. B. Reddy, Handbook of Batteries, Third Edition, McGraw Hill, New York, **2002**.

국문요약

수계 배터리 시스템은 물을 기반으로 한 전해질을 사용하기 때문에 폭발 위험성이 적고 유계 전해질보다 훨씬 경제적인 물을 사용하기 때문에 안정성과 경제성에서 큰 장점이 있다. 하지만 물의 전기화학적 안정성이 낮다는 큰 단점이 있다. 표준수소전극 대비 0 V 이하에서는 물이 환원되고 1.23 V 이상에서는 물이 산화되기 때문에 안정적으로 구동시킬 수 있는 범위가 1.23 V로 제한되기 때문이다. 이러한 이유로 고 에너지 밀도, 고 출력이 요구되는 배터리 중 대부분이 유계 전해질을 사용하고 있다. 이러한 수계 배터리의 단점을 보완할 수 있는 시스템으로 수계 리튬 배터리 시스템이 있다. 수계 리튬 배터리 시스템은 음극을 리튬으로 사용함으로써 수계 배터리의 전압을 대폭 상승 시킬 수 있다.

본 연구에서는 수계 리튬 배터리 시스템을 구현하기 위해 이에 맞는 셀 시스템을 제작하였고, 두 가지 실험 목표에 착안하여 연구를 진행하였다. 첫 번째 목표는 전위금속 이온 당 두개의 전자가 사용되는 $Ni^{2+}/Ni_{(s)}$ 산화환원 반응을 이용하여 용량을 높이는 것, 그리고 두 번째 목표는 높은 전압을 가지면서 동시에 값 싼 Fe^{3+}/Fe^{2+} 산화환원 반응을 이용하는 것이다.

계획했던 산화환원 반응은 XRD, SEM, 그리고 GITT 를 통해 분석하였다. 이러한 새로운 산화환원 반응을 통해 우리는 $Ni^{2+}/Ni_{(s)}$ 반응에서 높은 용량을 얻을 수 있었고, Fe^{3+}/Fe^{2+} 반응을 통해 높은 전압을 얻을 수 있었다.

주요어: 수계 리튬 배터리, Ni-Li 배터리, Fe-Li 배터리, 새로운 셀 시스템, 다양한 셀 반응

학 번: 2012-20603